Optics Communications 285 (2012) 2956–2960

Contents lists available at SciVerse ScienceDirect

Optics Communications

journal homepage: www.elsevier.com/locate/optcom

Four-wave mixing: Photon statistics and the impact on a co-propagating quantum signal

Álvaro J. Almeida [a,b,*], Nuno A. Silva [a,c], Paulo S. André [a,b], Armando N. Pinto [a,c]

[a] Instituto de Telecomunicações, Campus Universitário de Santiago, 3810-193 Aveiro, Portugal
[b] Department of Physics, University of Aveiro, Campus Universitário de Santiago, 3810-193 Aveiro, Portugal
[c] Department of Electronics, Telecommunications and Informatics, University of Aveiro, Campus Universitário de Santiago, 3810-193 Aveiro, Portugal

ARTICLE INFO

Article history:
Received 14 October 2011
Received in revised form 20 December 2011
Accepted 4 February 2012
Available online 21 February 2012

Keywords:
Photon statistics
Four-wave mixing
Maximum-likelihood estimation
Avalanche photodiodes

ABSTRACT

We reconstruct the photon statistics of a single-photon source based on the stimulated four-wave mixing (FWM) process. We find that the statistics of the source goes from thermal, at a low power regime, to Poissonian, at a high power regime. We also study the impact of the FWM process on a co-propagating coherent quantum signal in a wavelength-division multiplexed (WDM) lightwave system. The statistics of the quantum signal changes from Poissonian to thermal when a low power is used, and remains Poissonian for a higher power. A multithermal regime is also observed when a moderate power is used.

1. Introduction

The characterization of the photon statistics provides fundamental information on the nature of a source, which can be useful for quantum communications [1]. This characterization has been performed using different techniques [2–8]. In [2], a method based on quantum tomography for measuring the photon statistics of twin beams emerging from a nondegenerate optical parametric oscillator was presented. Using that method, the statistical characterization of the amplified signal at the fiber-optic parametric amplifier (FOPA) output was performed [3]. This technique requires phase-matching with a local oscillator and homodyne detection [6,9–12]. In [4], time-multiplexing techniques were used to obtain photon-number resolution using on/off detectors. These techniques allow to estimate the number of photons of an incident coherent state. Photomultiplier tubes were also employed to characterize the statistics of quantum states in the continuous-variable regime [5]. A different approach to estimate the photon statistics of an optical source was recently presented [6]. In that work, on/off avalanche photodetectors operating in the Geiger mode, assisted by the maximum-likelihood estimation (MLE) method and the expectation-maximization (EM) algorithm were used.

The coexistence of quantum and classical signals in a WDM lightwave system was recently demonstrated [13]. However, to the best of our knowledge, the evolution of the quantum signal photon statistics in these systems remains an open issue. The knowledge of the photon statistics is important in quantum communication networks, since the quantum bit-error rate (QBER) depends on this statistics [3,14].

In this work, we employ an on/off photodetector assisted by the MLE method and the EM algorithm [6], in order to numerically reconstruct the photon statistics of a single-photon source based on the stimulated FWM process in optical fibers. We also analyze the impact of the FWM process on a coherent quantum signal, co-propagating on a WDM lightwave system.

This paper contains four sections. In Section 2 we present the schematics of the experimental setup used, along with the numerical reconstruction method and the theoretical method used to adjust the reconstructed data. In Section 3, we report on the reconstruction of the photon statistics for two different cases. First, the statistics of the single-photon source based on the stimulated FWM process, and second the statistics of a co-propagating coherent quantum signal in the presence of FWM. The main results presented in this paper are summarized in Section 4.

2. Measurement method

In Fig. 1, we present the schematics of the experimental setup used for two different tasks: to determine the statistics of the idler photons generated from a single-photon source based on the stimulated FWM process [15–17], and the impact of the stimulated FWM process on the statistics of a coherent quantum signal, co-propagating in the system.

In order to determine the statistics of the photons generated from the stimulated FWM process, a pump at $\lambda_p = 1550.92$ nm, from a continuous-wave (CW) tunable laser source, was multiplexed with

* Corresponding author at: Instituto de Telecomunicações, Campus Universitário de Santiago, 3810-193 Aveiro, Portugal. Tel.: +351 234 377 900; fax: +351 234 377 901.
E-mail address: aalmeida@av.it.pt (Á.J. Almeida).

0030-4018/$ – see front matter © 2012 Elsevier B.V. All rights reserved.
doi:10.1016/j.optcom.2012.02.008

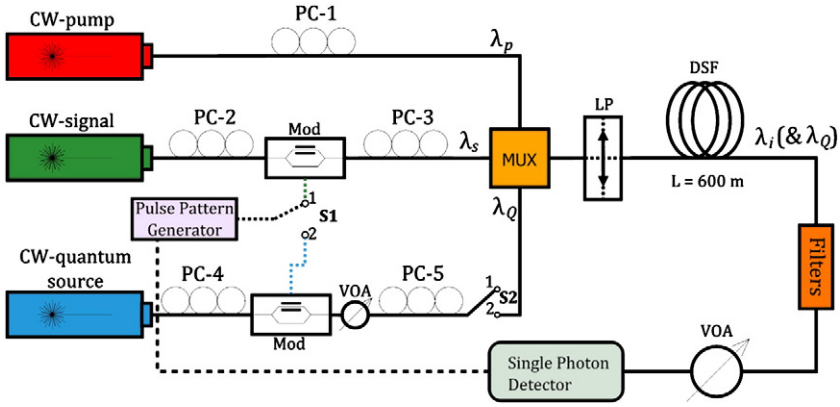

Fig. 1. Schematics of the experimental setup. The dashed lines represent electrical signals and the solid lines the optical path. The switches (S1 and S2) are used to change between the modulation of the classical signal (path 1) and the quantum source (path 2).

a signal from an external cavity laser centered at $\lambda_s = 1547.72$ nm. The signal field was pulsed with a full-width at half maximum (FWHM) of approximately 1 ns and a repetition rate of 1.22 MHz (path 1 in Fig. 1). The polarization controllers (PC) and the linear polarizer (LP) were used to send both fields co-polarized to the dispersion-shifted fiber (DSF), where an idler wave was generated at $\lambda_i = 1554.13$ nm. The DSF is characterized by a nonlinear parameter $\gamma = 2.3\ \mathrm{W^{-1}km^{-1}}$, zero-dispersion wavelength $\lambda_0 \approx 1550$ nm, and length $L = 600$ m. At the output of the fiber, the pump photons and the signal photons generated from the FWM process were suppressed by two cascaded flat-top dense wavelength-division multiplexing (DWDM) optical filters with a FWHM of 100 GHz, which provide a total isolation of about 100 dB. The idler photons passed through the filters and reached a variable optical attenuator (VOA) and a single photon detector module (SPDM), model id201 from ID Quantique, operating in the Geiger mode [18]. In the SPDM, a gate duration of 5 ns was employed, and the deadtime was set as 10 μs in order to avoid afterpulses. The quantum detection efficiency and the probability of having dark counts in the SPDM were measured as $\eta_D = 7.1\%$ and $P_{\mathrm{dc}} = 2.55 \times 10^{-5}$, respectively.

To study the impact of the FWM process on a co-propagating coherent quantum signal, with the same wavelength of the idler photons $\lambda_Q = \lambda_i$ (path 2 in Fig. 1), the quantum signal was multiplexed with the signal and the pump, and all signals were sent co-polarized to the DSF. By controlling the attenuation in the VOA, we can reach a state where the average number of photons per pulse is very low, i.e. of the order of 0.2. In the context of quantum key distribution (QKD), that optical field with such a low average number of photons per pulse is named as a quantum channel.

2.1. Numerical reconstruction method

The numerical method used for reconstructing the photon statistics through on/off detection (click/no-click events) was described in [6,19]. The statistics of no-click events from the SPDM, p_ν^{off}, is given by

$$p_\nu^{\mathrm{off}}(\eta_\nu) = (1-P_{\mathrm{dc}}) \sum_{n=0}^{N} (1-\eta_\nu)^n \rho_n, \tag{1}$$

where η_ν is the value of the combined efficiencies of the SPDM and the VOA, and ρ_n is the probability to obtain n photons. The solution for ρ_n can be obtained by the MLE method, through the EM algorithm [6] according to

$$\rho_n^{(i+1)} = \frac{\rho_n^{(i)}}{\sum_{j=1}^{K} A_{jn}} \sum_{\nu=1}^{K} f_\nu \frac{A_{\nu n}}{p_\nu^{\mathrm{off}}\left[\left\{\rho_n^{(i)}\right\}\right]}, \tag{2}$$

where $A_{\nu n} = (1-P_{\mathrm{dc}})(1-\eta_\nu)^n$, f_ν denotes the experimental frequencies of the no-click events for the efficiency η_ν, and $p_\nu^{\mathrm{off}}[\{\rho_n^{(i)}\}]$ is the no-click probability with quantum efficiency η_ν, obtained from the reconstructed distribution $\{\rho_n^{(i)}\}$. In our algorithm, we set the upper limit in the sum (Eq. (1)) to $N = K - 1 = 30$, where K is the number of different combined efficiencies considered. This allows the verification of normalization condition $\sum_{n=0}^{N} \rho_n \approx 1$. Note that even when the quantum efficiency of the detector is low, 7.1% in our case, the reconstruction of the photon statistics can be achieved with this method with very high values of fidelity [20].

2.2. Theoretical model

In order to compare the numerical reconstructed data with a theoretical model, a multimode field equation that combines coherent and thermal light can be used [11,21,22]. This equation, that represents the convolution of M thermal states, allows to obtain the photon distribution that have the form

$$\rho_n(n_{\mathrm{th}}, \alpha, M) = \frac{n_{\mathrm{th}}^n}{(1+n_{\mathrm{th}})^{n+M}} \exp\left(-\frac{|\alpha|^2}{1+n_{\mathrm{th}}}\right) \times L_n^{M-1}\left(-\frac{|\alpha|^2}{n_{\mathrm{th}}(1+n_{\mathrm{th}})}\right), \tag{3}$$

where $L_n^a(z)$ are the generalized Laguerre polynomials [11]. The parameter n_{th} represents the average number of thermal photons in each thermal state, and $|\alpha|^2$ is the average number of coherent photons [11,21,23]. Note that, if $n_{\mathrm{th}} < 0$ we are in the presence of a stimulated process [11].

From Eqs. (1) and (3), the no-click probability can be written as [11]

$$p_\nu^{\mathrm{off}}(\eta_\nu, n_{\mathrm{th}}, \alpha, M) = (1-P_{\mathrm{dc}}) \sum_{n=0}^{\infty} (1-\eta_\nu)^n \rho_n(n_{\mathrm{th}}, \alpha, M) = (1-P_{\mathrm{dc}}) \frac{1}{(1+\eta_\nu n_{\mathrm{th}})^M} \exp\left(-\frac{\eta_\nu |\alpha|^2}{1+\eta_\nu n_{\mathrm{th}}}\right). \tag{4}$$

From Eq. (4), two different cases arise. The first case is verified when $n_{\mathrm{th}} \to 0$, which gives a Poissonian statistics. The second one traduces a thermal statistics that appears when $\alpha \to 0$. The average number of photons at the fiber output according with Eq. (4), is $\mu = M n_{\mathrm{th}} + |\alpha|^2$, where $M n_{\mathrm{th}}$ is the expectation value of the photons in M thermal states [11,24,23].

As a measure of accuracy between the reconstructed and the theoretical distributions we adopt the fidelity, that can be defined as

$$G = \sum_{n=0}^{N} \sqrt{\rho_n \rho_n^{(N_i)}}, \tag{5}$$

where ρ_n is the theoretical distribution, and $\rho_n^{(N_i)}$ is the numerically reconstructed distribution, obtained at the last iteration $N_i = 1.22\times10^6$, with the number of iterations equal to the pulse rate [6,11].

3. Reconstruction of the photon statistics

In this section, we present the reconstruction of the photon statistics for the two cases under study. First, the photons generated from a single-photon source based on the stimulated FWM process. In the second case, we have sent to the DSF a coherent quantum signal co-propagating with the other two signals. We measured the photon statistics of the quantum signal at different powers, when it was subjected to interaction with the FWM process, i.e., when it carried different average numbers of photons.

3.1. Photon statistics of the stimulated FWM process

The schematic of the setup used in this experiment is presented in Fig. 1, considering path 1. First, we started by measuring the single-photon counts in the SPDM as a function of the VOA efficiency. Next, we have reconstructed numerically the experimental data by using the algorithm described in Section 2.1, for three different signal powers, considering the pump power fixed.

In Fig. 2, we present the reconstructed photon statistics using Eq. (2) and the correspondent comparison with Eq. (3). The no-click probabilities (p_ν^{off}) obtained from Eq. (1), and the best theoretical fits given by Eq. (4) are also plotted.

From Fig. 2(a)–(c), we can see that the statistics of the idler photons is quite dependant on the fiber input signal power. In Table 1 we display the values for $|\alpha|^2$, n_{th}, M, μ and G, for each case presented in

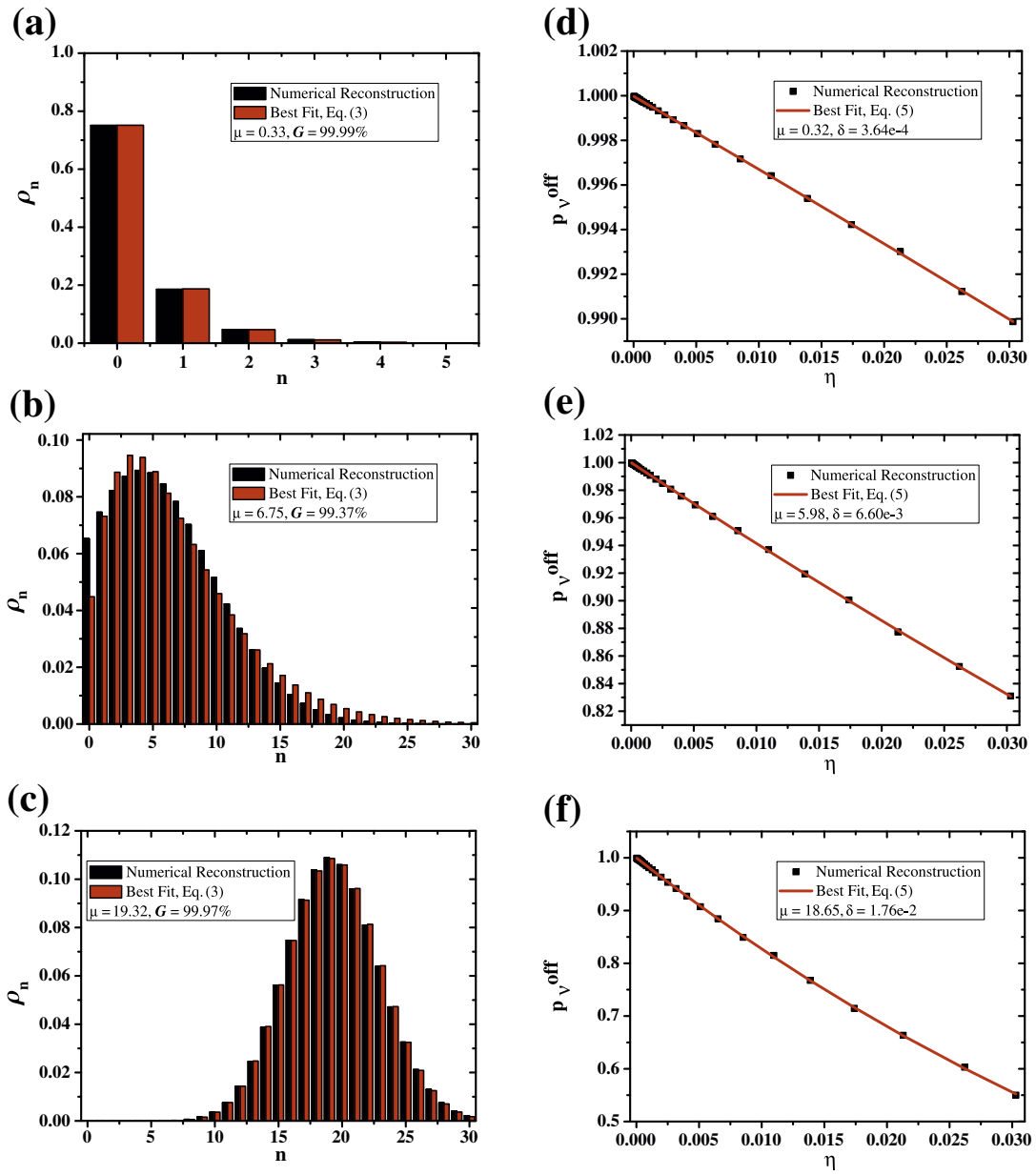

Fig. 2. Data obtained for the reconstruction of the statistics of a single-photon source based on the stimulated FWM process. Left side: Reconstructed photon statistics obtained from Eq. (2) (black bars), and best fits with Eq. (3) (red bars). The average number of photons (μ) and the fidelity (G), given by Eq. (5), are also presented. Right side: No-click probabilities (p_ν^{off}) obtained from Eq. (1) (black squares), and theoretical fit given by Eq. (4) (red line). The average number of photons (μ) and the error deviation (δ) are also presented. The pump power at the input of the fiber presented the value $P_p(0) = 2.63$ mW, and the signal powers at the input of the fiber were $P_s(0) = 0.12$ μW in (a) and (d), $P_s(0) = 0.01$ mW in (b) and (e), and $P_s(0) = 0.06$ mW in (c) and (f).

Table 1
Parameters obtained from the fit to Fig. 2(a), (b) and (c).

Figure	$\|\alpha\|^2$	n_{th}	M	μ	G [%]
2(a)	4.13×10^{-9}	0.33	1	0.33	99.99
2(b)	2.69	2.03	2	6.75	99.37
2(c)	21.24	−0.15	13	19.32	99.97

Fig. 2(a)–(c). From the analysis of Table 1 and Fig. 2, we can see that for the first case, Fig. 2(a), all the idler photons that emerge from the fiber obeys to a thermal statistics, since $|\alpha|^2 \to 0$ and $M = 1$. From Fig. 2(b) we can observe both thermal and coherent photons, taking into account n_{th} and $|\alpha|^2$ values, which indicates the presence of a multithermal statistics. For the last case, Fig. 2(c), we can observe a majority of coherent idler photons at the fiber output, due to stimulated processes. An increase in the number of thermal modes is verified as the signal power is increased. This arises from the fact that stimulated processes increasingly dominate. From the fidelity values G, a high accuracy between the reconstructed data and the theoretical fit can be observed.

In Fig. 2(d)–(f), we present the no-click probabilities (p_ν^{off}) given by Eq. (1) as a function of the combined efficiencies of the VOA and the SPDM, and the best theoretical fits obtained from Eq. (4). A good agreement between the reconstructed data and the theory is observed for each case presented in Fig. 2(d)–(f). That is observed also

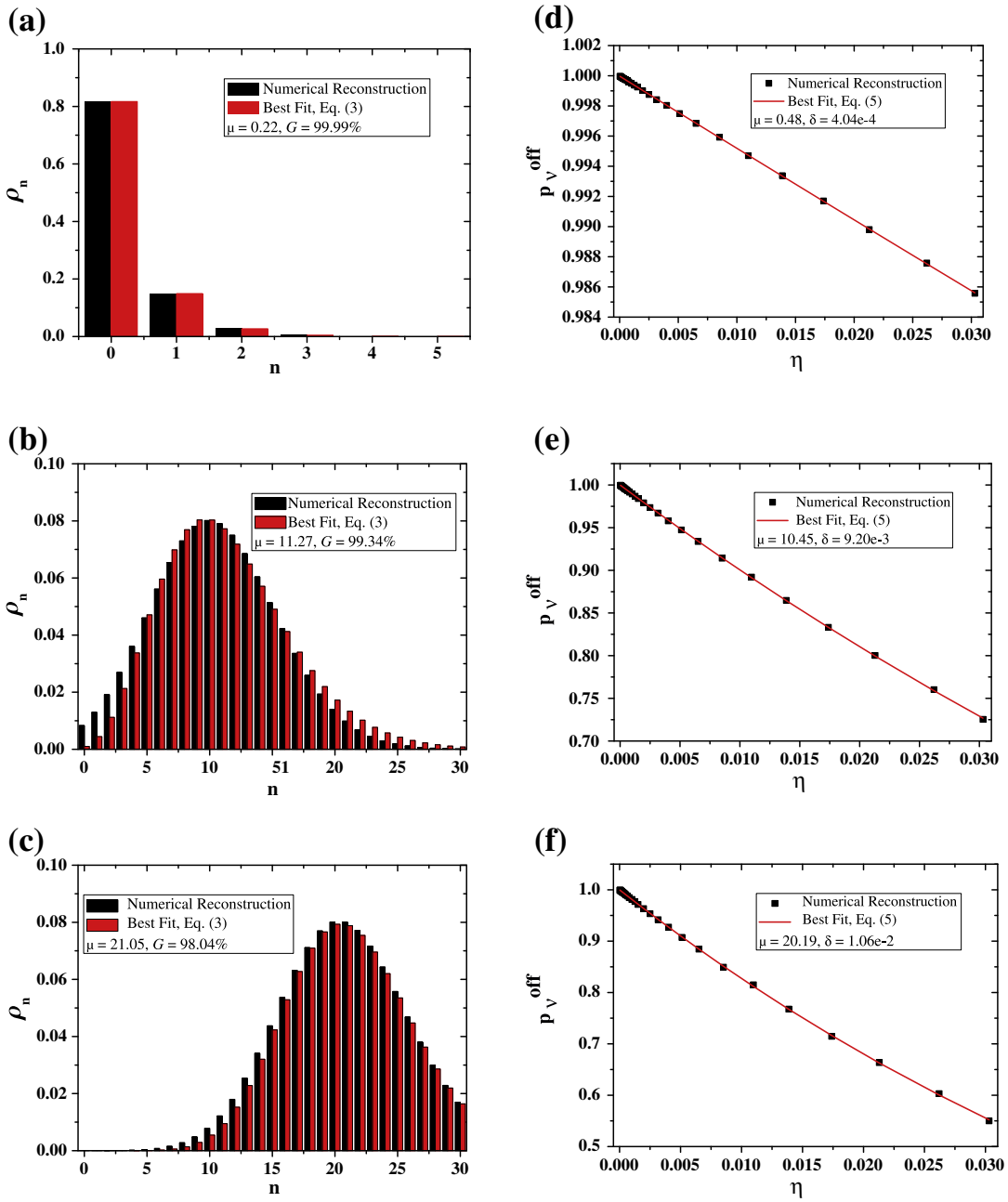

Fig. 3. Data obtained for the reconstruction of the statistics of a quantum signal when it was in the presence of the FWM process. Left side: Reconstructed photon statistics obtained from Eq. (2) (black bars), and best fits using Eq. (3) (red bars). The average number of photons (μ) and the fidelity (G), given by Eq. (5), are also presented. Right side: No-click probabilities (p_ν^{off}) obtained from Eq. (1) (black squares), and theoretical fits given by Eq. (4) (red line). The average number of photons (μ) and the error deviation (δ) are also presented. The pump and signal powers at the input of the fiber were $P_p(0) = 1.48$ mW and $P_s(0) = 0.06$ mW, and the quantum signal power at the input of the fiber presented the values, $P_Q(0) = 0.10$ nW in (a) and (d), $P_Q(0) = 5.20$ nW in (b) and (e), and $P_Q(0) = 6.76$ nW in (c) and (f).

Table 2
Parameters obtained from the fit to Fig. 3(a), (b) and (c).

Figure	$\|\alpha\|^2$	n_{th}	M	μ	G [%]
3a	1.61×10^{-8}	0.22	1	0.22	99.99
3b	7.08	0.84	5	11.27	99.34
3c	18.72	0.11	21	21.05	98.04

from the deviation (δ) between numerically reconstructed and theoretical data.

From these results, we can conclude that in a low power regime, the idler photons from the single-photon source based on the stimulated FWM process follow a thermal statistics. With the increase on the power, it changes to a multithermal statistics, until it finally reaches a Poissonian statistics, in a high power regime. The thermal statistics obtained arises from the spontaneous processes that dominate in that low power regime. Moreover, in a high power regime the stimulated processes dominate, and a Poissonian statistics from coherent states is obtained at the fiber output [3,22].

3.2. Impact of FWM on a co-propagating coherent quantum signal

In order to study the impact of the FWM process on the statistics of a co-propagating coherent quantum signal, we have used the scheme presented in Fig. 1, considering path 2. The modulated quantum signal is obtained from an attenuated laser source, and presents a Poissonian statistics at the fiber input [6,24,22]. The numerical method applied was the same as described previously, using the same efficiency values and the same number of iterations. The quantum signal was sent at the same wavelength where the idler photons were generated, in order to study the worst case scenario of interference. The pump and signal powers presented the values $P_p(0)=1.48$ mW and $P_s(0)=0.06$ mW, and the quantum source power was set as $P_Q(0)=0.10$ nW, $P_Q(0)=5.20$ nW, and $P_Q(0)=6.76$ nW.

In Fig. 3, we present the reconstructed photon statistics obtained from Eq. (2) and the correspondent comparison with Eq. (3). The no-click probabilities (p_ν^{off}) are also presented in Fig. 3 along with the best theoretical fits obtained with Eq. (4). From Fig. 3(a)–(c), we can see that the statistics of the photons of the quantum signal depends on its power at the input of the fiber. In Table 2 we present the values for $|\alpha|^2$, n_{th}, M, μ and G, for each case.

From Table 2 and Fig. 3, we can see for the first case, Fig. 3(a), where $P_Q(0)=0.10$ nW, that all the photons are thermal, taking into account that $|\alpha|^2\to0$ and $M=1$. This indicates that the statistics of the quantum signal changed from Poissonian to thermal after co-propagation with other classical signals. Increasing the power on the quantum signal, Fig. 3(b), a multithermal statistics verified from $|\alpha|^2$ and n_{th} values is observed. For $P_Q(0)=6.76$ nW, Fig. 3(c), it is seen that the majority of the photons are coherent, and only a few are thermal, since $|\alpha|^2\gg n_{th}$, with $|\alpha|^2=18.72$ and $n_{th}=0.11$, and in this case the multithermal statistics can be replaced by a Poissonian. As for previous case, described in Section 3.1, an increasing in the value of M with the quantum signal power increasing is verified, leading to a stimulated-photon regime. The high fidelity values obtained (G) confirms the accuracy between numerically reconstructed data and theoretical distributions.

In Fig. 3(d)–(f), we present the no-click probabilities (p_ν^{off}) given by Eq. (1) as a function of the combined efficiencies of the VOA and the SPDM, and the best theoretical fits obtained from Eq. (4). The reconstructed data and the theoretical no-click probabilities agree with high accuracy, as can be seen from the deviation values δ.

According with these results, we can conclude that when the quantum signal is driven in a low power regime, as in Fig. 3(a), its statistics changes from Poissonian to thermal, when it interacts with other classical signals through the FWM process. With the increase on the power of the quantum signal, the Poissonian statistics maintains, since the stimulated processes dominate all the process of generating photons inside the fiber.

4. Conclusion

We have presented a numerical reconstruction of the statistics of a single-photon source based on the stimulated FWM process. The reconstruction was performed using the MLE method, through the EM algorithm, and the data were obtained with a SPDM.

The reconstructed data were compared with a theoretical model based on the Laguerre statistics that used generalized Laguerre polynomials. Results have shown that in a low power regime, the distribution of the photons obeys to a thermal statistics. Increasing the power of the signal leads to a multithermal statistics that converges to a Poissonian statistics in a high power regime.

Regarding the impact of the FWM process on the statistics of a co-propagating coherent quantum signal, we establish that when the quantum signal is set at a low power regime, its statistics changes from Poissonian, at the fiber input, to thermal at the fiber output. With the increase on the power of the quantum signal, a multithermal statistics is verified. In a higher power regime it was verified that the quantum signal does not change its statistics, since it remains Poissonian at the input and at the output of the fiber. These results clearly show the need to mitigate the FWM process in WDM lightwave systems, in order to support quantum channels.

Acknowledgments

This work was supported in part by the FCT - Fundação para a Ciência e a Tecnologia, through the Ph.D. Grants SFRH/BD/79482/2011 and SFRH/BD/63958/2009, by the FCT and European Union FEDER - Fundo Europeu de Desenvolvimento Regional, through project 'QuantPrivTel'-PTDC/EEA-TEL/103402/2008, and by the FCT and the Instituto de Telecomunicações, under the PEst-OE/EEI/LA0008/2011 program, project 'P-Quantum'.

References

[1] N. Gisin, G. Ribordy, W. Tittel, H. Zbinden, Reviews of Modern Physics 74 (2002) 145.
[2] Y. Zhang, K. Kasai, M. Watanabe, Optics Letters 27 (14) (2002) 1244.
[3] P.L. Voss, R. Tang, P. Kumar, Optics Letters 28 (7) (2003) 549.
[4] M.J. Fitch, B.C. Jacobs, T.B. Pittman, J.D. Franson, Physical Review A 68 (4) (2003) 043814.
[5] G. Zambra, M. Bondani, A.S. Spinelli, F. Paleari, A. Andreoni, The Review of Scientific Instruments 75 (2004) 2762.
[6] G. Zambra, A. Andreoni, M. Bondani, M. Gramegna, M. Genovese, G. Brida, A. Rossi, M.G. Paris, Physical Review Letters 95 (6) (2005) 063602.
[7] B. Lounis, M. Orrit, Reports on Progress in Physics 68 (2005) 1129.
[8] M. Oxborrow, A.G. Sinclair, Contemporary Physics 46 (2005) 173.
[9] M. Genovese, M. Gramegna, G. Brida, M. Bondani, G. Zambra, A. Andreoni, A.R. Rossi, M.G.A. Paris, Laser Physics 16 (2006) 385.
[10] G. Zambra, M.G.A. Paris, Physical Review A 74 (6) (2006) 063830.
[11] G. Brida, M. Genovese, A. Meda, S. Olivares, M.G.A. Paris, F. Piacentini, Journal of Modern Optics 56 (2009) 196.
[12] G. Brida, M. Genovese, M. Gramegna, A. Meda, F. Piacentini, P. Traina, E. Predazzi, S. Olivares, M.G. Paris, Advanced Science Letters 4 (1) (2011) 1.
[13] T.J. Xia, D.Z. Chen, G. Wellbrock, A. Zavriyev, A.C. Beal, K.M. Lee, Optical Fiber Communication Conference and Exposition and The National Fiber Optic Engineers Conference, Optical Society of America, 2006, p. OTuJ7.
[14] N.J. Muga, M.F.S. Ferreira, A.N. Pinto, Journal of Lightwave Technology 29 (3) (2011) 355.
[15] N.A. Silva, N.J. Muga, A.N. Pinto, Journal of Lightwave Technology 27 (22) (2009) 4979.
[16] N.A. Silva, N.J. Muga, A.N. Pinto, IEEE Journal of Quantum Electronics 46 (3) (2010) 285.
[17] N.A. Silva, N.J. Muga, A.N. Pinto, Optics Communications 284 (13) (2011) 3408.
[18] G. Ribordy, N. Gisin, O. Guinnard, D. Stucki, M. Wegmuller, H. Zbinden, Journal of Modern Optics 51 (2004) 1381.
[19] D. Mogilevtsev, Optics Communications 156 (1998) 307.
[20] A.R. Rossi, M.G.A. Paris, European Physical Journal D: Atomic, Molecular, Optical and Plasma Physics 32 (2) (2005) 223.
[21] B.R. Mollow, R.J. Glauber, Physical Review 160 (1967) 1076.
[22] M. Martinelli, P. Martelli, Optics & Photonics News 19 (2) (2008) 30.
[23] R. Noé, Electrical Engineering (Archiv fur Elektrotechnik) 83 (2001) 15.
[24] T. Li, M.C. Teich, IEEE Journal of Quantum Electronics 29 (1993) 2568.